Network Deployment for ATG Communications: A Cell-Free Approach Under the Hybrid Satellite-Terrestrial Network Architecture

Qinzhao Zhang ⬤, Jue Wang ⬤, *Member, IEEE*, Ruifeng Gao ⬤, *Member, IEEE*, Yanmin Wang ⬤, and Wei Feng ⬤, *Senior Member, IEEE*

Abstract—Due to the increasing demand for Internet access on aircraft, air-to-ground (ATG) communications have recently received extensive attention. Determining the locations of ATG base stations (BSs) is an important guarantee for efficient ATG communications. To this end, we consider an aircraft-centric ATG network where the aircraft is served by its adjacent ATG BSs. For this scenario, we formulate an optimization problem to determine the best number and locations of ATG BSs, to maximize the average uplink channel capacity. The problem is shown to be discontinuous and nonconvex. To tackle this challenge, we first propose a stochastic subgradient-based method to determine the locations of ATG BSs, followed by an algorithm to further determine the minimum number of BSs that satisfies the communication requirements on the target routes. Due to the nonconvexity of the problem, the solution obtained by stochastic optimization is not unique. To address this issue, we further propose a clustering method to obtain a unique solution for practical implementation. Simulation results confirm the effectiveness of our proposed algorithm compared with existing ATG BS deployment methods.

Index Terms—Air-to-ground (ATG), base station (BS) location, cell-free, channel capacity, clustering method, stochastic subgradient.

Qinzhao Zhang and Wei Feng are with the Department of Electronic Engineering, Beijing National Research Center for Information Science and Technology, Tsinghua University, Beijing 100084, China (e-mail: zqz20@mails.tsinghua.edu.cn; fengwei@tsinghua.edu.cn).

Jue Wang is with the School of Information Science and Technology, Nantong University, Nantong 226019, China, and also with the Nantong Research Institute for Advanced Communication Technology, Nantong 226019, China (e-mail: wangjue@ntu.edu.cn).

Ruifeng Gao is with the School of Transportation and Civil Engineering, Nantong University, Nantong 226019, China, and also with the Nantong Research Institute for Advanced Communication Technology, Nantong 226019, China (e-mail: grf@ntu.edu.cn).

Yanmin Wang is with the School of Information Engineering, Minzu University of China, Beijing 100041, China (e-mail: yanmin-226@163.com).

I. INTRODUCTION

AS AN important scenario for future ubiquitous wireless coverage, providing Internet access to aircraft has attracted considerable attention from both academia and industry. Currently, there are mainly two methods to enable network connectivity on aircraft: satellite communications [1] and air-to-ground (ATG) communications [2]. Satellite communications can provide worldwide service, however, they suffer from high costs, large delay and path loss, and limited bandwidth. Alternatively, ATG communications deploy dedicated ground base stations (BSs) (termed ATG BSs) to enable direct data transmission to the aircraft. Compared with satellite, ATG communications have the advantages of better communication performance and lower implementation cost, but also with a much smaller coverage area. To fully exploit the benefits of both methods, the hybrid satellite–terrestrial network architecture [3], [4], [5], [6], [7], [8], [9], [10], [11] has been proposed, which can service aircraft using a strong terrestrial ATG network when available, and achieve full coverage using satellite in the areas where ATG BSs cannot be established. Specifically, the civil aircraft-enabled space–air–ground integrated network has been studied in [9], [10], and [11]. In addition, Fang et al. [12] proposed a combination weighting evaluation model to determine the congestion status of the ATG network, and accordingly prevent node failures and reduce routing network congestion. Tian et al. [13] proposed a lightweight group preswitching authentication scheme suitable for aviation 5G ATG networks, which reduces the security risks of users switching between ATG BSs and reduces computational overhead. Papa et al. [14] discussed possible aviation applications in the 6G era and proposed an aviation alliance framework to integrate aviation communications into 6G. The existing works indicate that efficient construction of the ATG network, in such a hybrid architecture, plays an important role in enabling high-performance in-flight connectivity.

Determining BS locations is important for efficient ATG network construction. ATG BSs need to be deployed reasonably to cover aircraft users on sparse and unevenly distributed routes. In addition, the construction cost of ATG BSs is relatively high, and hence, it is important to optimize the location of ATG BSs to reduce the required number of BSs and save cost. In general, the ATG BSs should be deployed by jointly considering the aircraft distribution and communication requirements

on the target routes. A carefully designed network topology (more specifically, the BS locations) can improve the system performance while reducing the implementation cost. For terrestrial networks, the problem of BS placement (or in other terms, coverage optimization, cell planning, etc.) has long been investigated [15], [16], [17]. However, these methods usually aim at providing full coverage of a target area, wherein the users are usually assumed to be uniformly distributed. This may be a valid assumption in conventional terrestrial cellular scenarios, but it becomes different in the scenario of ATG communications. The objective of coverage becomes lines (routes) instead of an area, and users (aircraft) now follow 1-D distribution on their corresponding routes, instead of uniformly distributed in the whole space. Therefore, conventional BS location optimization methods are no longer efficient.

User route information becomes a key issue that should be taken into account in the ATG BS deployment. There exists a similar scenario. High-speed railway communications, where the users (trains) also follow specific routes. The optimal deployment of railway BSs has been investigated in [18] and [19]. In these works, optimization of the inter-BS distance and the rail-BS distance is the focus. Although the user route information has been exploited in the design, unfortunately, those approaches still cannot be directly applied for ATG BS deployment. A major reason is that an ATG BS is supposed to cover a much larger (aero) area and hence it can serve multiple routes simultaneously, while this is not true for railways. The much wider coverage of ATG BSs admits their location optimization being conducted in a cell-free manner, that is, an aircraft can be cooperatively served by multiple adjacent BSs. This property, if exploited, can provide more degrees of freedom in the design, and make the ATG BS deployment more efficient. Therefore, new BS location optimization method dedicated to the ATG communications scenario is required.

Currently, there exist several ATG BS deployment methods using cellular layout [20], [21], [22], [23] to provide full coverage of the airspace above ground. Shaverdian et al. [20] discussed the use of airport cellular BSs to capture data generated during aircraft landing. Dinc et al. [21] and [22] proposed an analytical framework to analyze and optimize the total cost of ownership of the ATG network to provide coverage to European airspace. Towhidlou et al. [23] investigated the network handover problem in ATG communications for cellular-connected aircraft. These methods could be efficient for the scenario that routes are densely distributed, such that the aircraft distribution can be seen as approximately uniform (e.g., as released by the new generation mobile network alliance [24], it is 60 aircraft per 18 000 km^2). However, the distribution of routes in most regions of the world could be uneven and sparse in practice. For example, the routes in the eastern part of China are much denser than that in the western part. In this case, the existing cellular-based approaches become inefficient in terms of construction costs. To accommodate uneven routes, Cao et al. [25] proposed a hybrid genetic algorithm-particle swarm optimization (GA-PSO) algorithm for the BS location determination. Wang et al. [26] formulated the BS deployment problem in the form of a classical set coverage problem (SCP) and correspondingly proposed a solution. Although these methods

take into account practical route distribution, they are designed from the perspective of geometrical coverage without considering exact communication performance as an objective. Therefore, communication performance during flight might not be guaranteed.

To this end, we investigate the number and location optimization of ATG BSs, to serve unevenly distributed routes with given communication rate requirements. The contributions are summarized as follows.

1) We find an analytical expression for the ergodic channel capacity under the considered ATG communications scenario, with only large-scale fading coefficients (determined by the geographic coordinates of the aircraft and the ATG BSs) being parameters. After that, an optimization problem is formulated, aiming to find the best number and locations of ATG BSs to maximize the uplink channel capacity.

2) The problem is shown to be nonconvex with discontinuous constraints, for which we propose a two-step approach to solve it. First, we propose a stochastic subgradient-based algorithm to optimize the locations of ATG BSs for a fixed BS number; then, the algorithm is conducted iteratively to further determine the minimum ATG BS number that can meet the communication requirements on the target routes.

3) Due to the nonconvexity of the formulated problem, the solution obtained by stochastic optimization is not unique. Specifically, the obtained BS number and locations may be different in different runs due to random initialization. To tackle this problem, we further use a clustering method to cluster the BS locations obtained in multiple runs into different groups. The average coordinates of every BS group are then used to provide a unique solution for practical ATG BS implementation.

4) Extensive simulations are conducted to show the performance of the proposed ATG BS deployment algorithm. Compared with existing BS location determination methods, the proposed algorithm is shown to have a clear advantage in terms of not only the average uplink capacity but also the real-time capacity changing along the routes.

The rest of this article is organized as follows. In Section II, we describe the system model for the considered ATG communications system, followed by problem formulation. In Section III, a stochastic subgradient-based algorithm is proposed to solve the formulated problem. A clustering method is proposed in Section IV to tackle the problem of nonunique solutions. Simulation results are discussed in Section V. Finally, Section VI concludes this article.

II. SYSTEM MODEL AND PROBLEM FORMULATION

We consider an aircraft-centric ATG communications network, as shown in Fig. 1, where the aircraft flying along several fixed routes communicate with multiple ATG BSs. Adjacent BSs cooperatively serve the aircraft above, i.e., the network operates in a cell-free manner. The aircraft are randomly distributed on their corresponding routes, with a specific safety distance guaranteed between any two of them. All the aircraft and BSs are implemented with multiple antennas. For practical reasons (e.g.,
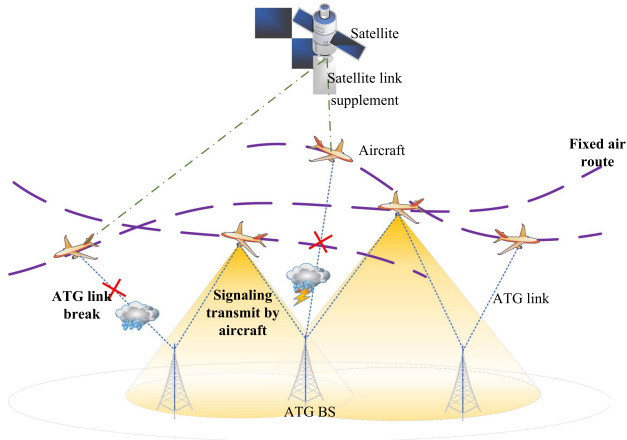
Fig. 1. Illustration of the cell-free ATG communications system under the hybrid satellite–terrestrial network architecture.

the climate), the aircraft might not always be able to connect with an ATG BS. When the ATG link is not available, the aircraft will turn to satellite as a supplement.

Consider that there are R routes, with J_r aircraft distributed on the rth route,[1] which need to be served by the ATG BSs. The total number of aircraft is $J = \sum_{r=1}^{R} J_r$, and each aircraft is equipped with N_A antennas. Assume the number of BSs is I,[2] and each BS has N_B antennas. We define $N \triangleq JN_A$, and $M \triangleq IN_B$, which are the total number of antennas at the aircraft side and the BS side, respectively. Consider the uplink (i.e., aircraft to BS), the baseband signal model for all aircraft and BSs can be written as[3]

$$\mathbf{y} = \mathbf{H}(\mathbf{c}^A, \mathbf{c}^B)\mathbf{x} + \mathbf{n} \qquad (1)$$

where $\mathbf{y} = [y_1, \ldots, y_M]^T$ represents the received signal vector, which is composed of the signals received by all BS antennas. $\mathbf{x} = [x_1, \ldots, x_N]^T$ represents the transmit signal vector composed of signals from all aircraft antennas, $\mathbf{n} = [n_1, \ldots, n_M]^T$ is the additive Gaussian white noise vector. $\mathbf{H} \in \mathbb{C}^{M \times N}$ is the channel matrix from the aircraft located at $\mathbf{c}^A$ to the BSs located at $\mathbf{c}^B$. Specifically, it can be expressed as $\mathbf{H} = \mathbf{S} \circ \mathbf{L}$, where $\circ$ denotes the Hadamard product. $\mathbf{S} \in \mathbb{C}^{M \times N}$ represents the small-scale fading matrix and its components $\mathbf{s}_{mn}$ are modeled as independent and identically distributed circularly symmetric complex Gaussian random variable with zero mean and unit variance. $\mathbf{L} \in \mathbb{C}^{M \times N}$ represents the large-scale fading matrix obtained from the path loss model, which is partitioned into

[1]In order to better fit the flight conditions of the aircraft on the actual route, we set the number of aircraft J_r on each route as a random variable, i.e., the value of J_r is uncertain in different snapshots of the network.

[2]Note that in our following analysis, the value of I is to be minimized to provide satisfactory coverage of the target routes with minimum cost.

[3]In the cell-free setting, an aircraft is served only by its adjacent ATG BSs. However, to facilitate analysis, the following signal model implies full connection between all BSs and aircraft. Note that in the scenario of ATG communications, the path loss between an aircraft and a faraway BS can be very large. Therefore, the capacity obtained with (1) can be viewed as a tight upper bound of the real uplink capacity achieved by cell-free transmissions.

$X = IJ$ submatrices as

$$\mathbf{L} = \begin{pmatrix} \mathbf{L}_{11} & \cdots & \mathbf{L}_{1J} \\ \vdots & \ddots & \vdots \\ \mathbf{L}_{I1} & \cdots & \mathbf{L}_{IJ} \end{pmatrix} \qquad (2)$$

where each submatrix $\mathbf{L}_{ij} \, \forall i = 1 \ldots I, j = 1, \ldots, J$ consists of all-same elements representing the path loss between the BS i and the aircraft j, determined only by the corresponding distance between these two nodes, d_{ij}. According to Nagawana and Miyazaki [27], we adopt the following ATG path loss model:

$$\gamma_{ij}[\text{dB}] = 20\log_{10}\left(\frac{4\pi f d_0 \times 10^9}{c}\right)$$
$$+ 10n_0\log_{10}\left(\frac{d_{ij}}{d_0}\right) + L_{\text{atm}} \qquad (3)$$

where f is the carrier frequency in mHz, $d_0 = 1\,\text{m}$ is the reference distance, $n_0 = 2$ is the free space path loss exponent, c is the speed of light, and L_{atm} is the atmospheric attenuation loss which value is $0.009\,\text{dB/NM}$ ($1\,\text{NM} = 1.852\,\text{km}$).

Assuming that all aircraft transmit with a constant signal power P and adopt equal power allocation among the antennas, the uplink ergodic channel capacity (normalized by the total number of BSs antennas) can be written as

$$C = \frac{1}{M}\mathbb{E}\left[\log_2 \det\left(\mathbf{I}_M + \frac{\rho}{N_A}\mathbf{H}\mathbf{H}^*\right)\right] \qquad (4)$$

where $\rho = \frac{P}{\sigma_0^2}$ is the transmit signal-to-noise ratio (SNR), and $(\cdot)^*$ means Hermitian transpose. Note that the normalization factor $\frac{1}{M}$ is added in (4), for the reason that the number of BSs is not fixed and is to be optimized in our considered scenario. Therefore, considering the perantenna capacity in (4) provides a fair objective.

With this system model in hand, our aim is to maximize the averaged perantenna uplink capacity in (4) (i.e., making the deployment of ATG BSs more efficient), while guaranteeing the capacity of every individual aircraft (on the target routes) larger than a given threshold, for smooth and satisfactory quality of service (QoS). For this purpose, the number and locations of ATG BSs are to be optimized, and (4) is averaged over all possible aircraft locations as the design objective. Denote $\mathbf{c}^B = [(x_1^B, y_1^B)^T, \ldots, (x_I^B, y_I^B)^T]$ as the location matrix of the ATG BSs, and denote $\mathbf{c}^A = [(x_1^A, y_1^A)^T, \ldots, (x_J^A, y_J^A)^T]$ as the location matrix of the aircraft, the optimization problem is then formulated as

$$\max_{\{\mathbf{c}^B\}} \left\{ \mathbb{E}_{\{\mathbf{c}^A\}} \left[C\left(\mathbf{c}^A, \mathbf{c}^B\right) \right] \right\}$$

$$\text{s.t.} \quad C_j \geqslant \Omega, j = 1 \ldots J \qquad (5)$$

where $C(\mathbf{c}^A, \mathbf{c}^B)$ is calculated using (4) with $\mathbf{c}^A$ and $\mathbf{c}^B$ as parameters, since the locations of BSs and aircraft directly affect the path loss calculation in (2) [and further, $\mathbf{H}$ in (4)]. Moreover, C_j is the uplink capacity of the jth aircraft,[4] and Ω is the

[4]In practice, C_j can be calculated as $\mathbb{E}[\log_2 \det(\mathbf{I}_{M_j} + \frac{\rho}{N_A}\mathbf{H}_j\mathbf{H}_j^*)]$ where M_j is the total number of BS antennas associated with aircraft j (in the cell-free setting), and $\mathbf{H}_j \in \mathbb{C}^{M_j \times N_A}$ is the corresponding submatrix of $\mathbf{H}$.

minimum capacity threshold to guarantee QoS. Note that the proposed problem (5) is described for a fixed number of BSs I. In practice, it is desirable to find the smallest I that satisfies all constraints.

The proposed problem will face the following three challenges.

1) The optimization parameters $\mathbf{c}^A$ and $\mathbf{c}^B$ are implicitly reflected in the expression of (4).
2) It is difficult to obtain a closed form expression for the expectation (over $\mathbf{c}^A$) in the objective function.
3) The minimization of I is coupled with the optimization of $\mathbf{c}^B$.

III. NUMBER AND LOCATION OPTIMIZATION FOR ATG BS DEPLOYMENT

We resort to the following methods to tackle the above challenges.

1) We find an approximation for (4), which relates the ergodic capacity C more closely to $\mathbf{c}^A$ and $\mathbf{c}^B$.
2) We propose a stochastic subgradient-based method to solve problem (5) for a fixed number of I.
3) An iterative algorithm is further proposed to identify the minimum I that satisfies the constraints in (5).

Details are described in the following.

A. Approximation of the Ergodic Uplink Capacity

We consider the asymptotic regime that the number of aircraft antennas and BS antennas satisfies $N_A \to \infty$, $N_B \to \infty$, and $\frac{N_A}{N_B} \to \beta$.[5] In this case, the capacity in (4) can be approximately expressed as [28]

$$C = \frac{1}{I} \sum_{i=1}^{I} \log_2 U_i + \frac{\beta}{I} \sum_{j=1}^{J} \log_2 W_j$$
$$- \frac{\rho \log_2 e}{I} \sum_{i=1}^{I} \sum_{j=1}^{J} \frac{\gamma_{ij}^2}{U_i W_j} \quad (6)$$

where γ_{ij} represents the large-scale channel fading coefficient between the ith BS and the jth aircraft, which can be directly obtained by (3) once d_{ij}, determined by $\mathbf{c}^A$ and $\mathbf{c}^B$, is given. Assuming that the total number of BS antennas is no less than the total number of aircraft antennas, i.e., $M \geqslant N$ and U_i and W_j are given as follows [29]:

$$U_i = \left(1 - \frac{\beta}{\rho I \Phi} F\left(\frac{\rho I \Phi}{\beta}, \frac{J\beta}{I} \right) \right)^{-1}, i = 1 \ldots I \quad (7)$$

$$W_j = 1 + \frac{\rho}{\beta} \sum_{i=1}^{I} \frac{\gamma_{ij}^2}{\left(1 - \frac{\beta}{\rho I \Phi} F\left(\frac{\rho I \Phi}{\beta}, \frac{J\beta}{I} \right) \right)^{-1}}, j = 1 \ldots J \quad (8)$$

with

$$F(x, z) = \frac{1}{4} \left(\sqrt{x\left(1 + \sqrt{z}\right)^2 + 1} - \sqrt{x\left(1 - \sqrt{z}\right)^2 + 1} \right)^2 \quad (9)$$

and

$$\Phi = \frac{1}{IJ} \sum_{i=1}^{I} \sum_{j=1}^{J} \gamma_{ij}^2. \quad (10)$$

Now, given $\mathbf{c}^A$ and $\mathbf{c}^B$, $d_{ij} \, \forall i, j$ can be calculated and so are $\gamma_{ij} \, \forall i, j$. Subsequently, U_i and W_j can be directly obtained with (7)–(10), and the capacity C is correspondingly calculated with (6). These approximations directly relate C to $\mathbf{c}^A$ and $\mathbf{c}^B$ via the above procedure and facilitate the following optimization design.

B. Stochastic Subgradient-Based BS Location Optimization (Fixed I)

Using the results derived above, we proceed to solve the maximization problem in (5) while somewhat relaxing the constraints at this stage. That is, we first try to find the optimal BS location deployment that maximizes $\mathbb{E}_{\{\mathbf{c}^A\}}[C(\mathbf{c}^A, \mathbf{c}^B)]$ for a fixed BS number, I. Note that when the value of I is set too small, it might be difficult to guarantee all J constraints ($C_j \leq \Omega, j = 1, \ldots, J$). Nonetheless, the optimization will be conducted in such a way, that the rate is maximized while guaranteeing as many constraints as possible. The problem is now described as

$$\max_{\{\mathbf{c}_I^B\}} \left\{ \mathbb{E}_{\{\mathbf{c}^A\}} C\left(\mathbf{c}^A, \mathbf{c}_I^B \right) \right\} \quad (11)$$

where subscripts I are added to $\mathbf{c}^B$ to highlight that the location coordinates, at this stage, are optimized under a fixed number of nodes.

As discussed earlier, it is difficult to express the expectation over random aircraft locations ($\mathbb{E}_{\{\mathbf{c}^A\}}[\cdot]$) in closed form. This makes the widely used optimization methods, such as successive convex approximation (SCA) [30], difficult to be applied for the reason that they in general need to construct deterministic convex functions without expectations. Therefore, we turn to use stochastic optimization methods to solve it by exploiting the known distribution information of the aircraft along the considered routes. Considering the discontinuity of channel capacity caused by the uncertain number of aircraft, we choose to utilize the stochastic subgradient method [31] to solve the problem. The corresponding iterative representation expression can be written as

$$\mathbf{c}_I^B(t+1) = \mathbf{c}_I^B(t) + \alpha(t)\mathbf{g_c}(t) \quad (12)$$

where $\mathbf{g_c}(t)$ is the subgradient of $C(\mathbf{c}^A, \mathbf{c}_I^B)$ (with respect to $\mathbf{c}_I^B$) at step t. $\alpha(t)$ is the step size that needs to satisfy

$$\alpha(t) \geq 0 \quad (13a)$$

$$\sum_t |\alpha(t)|^2 < \infty \quad (13b)$$

$$\sum_t |\alpha(t)| = \infty \quad (13c)$$

---

[5]Note that this asymptotic assumption is reasonable in the considered ATG communications scenario, since large antenna arrays are usually implemented at the ATG BSs and aircraft to compensate for the severe path loss from ATG [24]. Besides, as we are focusing the routes over a wide area, within which there may exist a large number of ATG BSs and aircraft. This further ensures a sufficiently large number of overall transmit/receive antennas in (4).

to guarantee convergence. In each iteration step described in (12), the algorithm will independently draw a realization of $\mathbf{c}_A$ according to its distribution, to approximately deal with the expectation term $\mathbb{E}_{\{\mathbf{c}^A\}}$ in (11). By iterating (12), the largest function value (and the corresponding $\mathbf{c}_I^{B*}$) is obtained as

$$C(\mathbf{c}_I^{B*}) = \max_{i=0,\dots,t} C(\mathbf{c}_I^B(i)). \tag{14}$$

Now, the key is to describe the subgradient matrix $\mathbf{g_c}(t)$ in (12). In our design, $\mathbf{g_c}(t)$ is composed of two parts as

$$\mathbf{g_c}(t) = \omega_{\mathbf{c}}(t) + \tilde{\omega}_{\mathbf{c}}(t) \tag{15}$$

where

$$\omega_{\mathbf{c}}(t) = \left. \frac{\partial C}{\partial \mathbf{c}_I^B} \right|_{\{\mathbf{c}_J^A(t), \mathbf{c}_I^B(t)\}} \tag{16}$$

is determined by calculating the partial derivative of C with respect to $\mathbf{c}_I^B$ and evaluate its value at $\{\mathbf{c}_J^A(t), \mathbf{c}_I^B(t)\}$, i.e., the coordinates matrix of J aircraft and I BSs at the tth step. The locations and number of aircraft here, at each iteration, are independently and randomly generated based on their distribution on the corresponding routes.

In addition, we introduce a modified subgradient term, $\tilde{\omega}_{\mathbf{c}}(t)$, to partially incorporate the QoS constraints in (5). This term is defined as follows:

$$\tilde{\omega}_{\mathbf{c}}(t) = \frac{1}{2} \sum_{j=1}^{N_q(t)} \frac{\Omega - C_j(t)}{N_q(t)\Omega - \sum C_j(t)} \left. \frac{\partial C_j(t)}{\partial \mathbf{c}_I^B} \right|_{\{\mathbf{c}_J^A(t), \mathbf{c}_I^B(t)\}} \tag{17}$$

where $N_q(t)$ is the total number of aircraft (at step t) whose QoS is not guaranteed at the current iteration step, $C_j(t)$ represents the uplink channel capacity of the jth aircraft that doesn't have its QoS satisfied at step t, and the term $\frac{\Omega - C_j(t)}{N_q(t)\Omega - \sum C_j(t)}$ is introduced as a weight coefficient to balance the searching direction among all the directions that tend to increase $C_j(t) \forall j$. Note that introducing $\tilde{\omega}_{\mathbf{c}}(t)$ in (15) does not necessarily mean that all QoS constraints must be satisfied at this stage. Actually, when the value of I is set small, satisfying all QoS constraints could be impossible. Nevertheless, this modified searching direction guarantees that in every iteration step, the updated BS locations tend to move closer to those routes on which the aircraft's QoS is less guaranteed.

Then, we further discuss the choice of step size $\alpha(t)$ in (12). We use the Adam algorithm [32] and correspondingly set $\alpha(t)$ as

$$\boldsymbol{\alpha}(t) = \frac{\lambda(t)}{\sqrt{\delta + \mathbf{V}(t)}} \tag{18}$$

where the constant δ is set to be a small and nonzero value to stabilize the step size. $\lambda(t) = \frac{a}{t^b}$ is the step size coefficient with $a > 0$ and $b > 0.5$, which can satisfy the three conditions in (13) to ensure convergence. $\mathbf{V}(t)$ is the second-order moment estimation of $\mathbf{g_c}(t)$ with bias correction, which is updated for each step as

$$\mathbf{V}(t) = \tau_1 \mathbf{V}(t-1) + \frac{(1-\tau_1)}{(1-\tau_1^t)} \mathbf{g_c}(t) \circ \mathbf{g_c}(t) \tag{19}$$

where $\tau_1 = 0.5$ is a decay factor for $\mathbf{V}(t-1)$.

On the other hand, we can modify the subgradient by using its first moment to smoothen the subgradient changing between two consecutive steps, which now becomes

$$\mathbf{S}(t) = \tau_2 \mathbf{S}(t-1) + \frac{(1-\tau_2)}{(1-\tau_2^t)} \mathbf{g_c}(t) \tag{20}$$

where $\tau_2 = 0.5$ is the decay factor for $\mathbf{S}(t-1)$.

For the initial iteration $t = 1$, we set $\mathbf{g_c}(t-1) = 0$ [i.e., $\mathbf{V}(-1) = 0$ and $\mathbf{S}(-1) = 0$ in (19) and (20)]. Finally, the iterative (12) to solve the proposed problem (11) is now realized as

$$\mathbf{c}_I^B(t+1) = \mathbf{c}_I^B(t) + \boldsymbol{\alpha}(t) \circ \mathbf{S}(t). \tag{21}$$

The iteration keeps updating the obtained BS locations, until that we can finally obtain a solution to problem (11) and get a locally optimal set of BS locations for a fixed value of I.

C. Identify the Minimum I

In the previous section, the algorithm tends to update the BS locations toward the routes, on which the QoS is less satisfied. However, when I is set too small, it might be impossible to guarantee the QoS at any arbitrary aircraft location for all the considered routes. Increasing I to a sufficiently large value can alleviate this problem, yet, the network operator would be more interested in finding the minimum I that can well cover all the routes in order to reduce construction costs. For this consideration, we further propose a method in this section to identify this minimum I.

For initialization, we first set I to a small value. For the current I, we obtain the BS locations using the stochastic subgradient-based method described above. Then, we traverse all possible aircraft locations $\mathcal{C}^A$ on all the considered routes,[6] calculate the corresponding channel capacity C_z for every aircraft location (obtained with the current optimized BS locations), and the ratio of satisfying QoS at the current sampling point ψ (i.e., the approximation of the probability, specifically, the quantity that satisfies $C_z \geqslant \Omega$, which represents the minimum capacity threshold). If the ratio is less than the target value $\Psi = 95\%$,[7] we will increase I and repeat the above procedure. The entire algorithm flow is described in Algorithm 1. The final output of the algorithm is the location set of the ATG BSs $\mathcal{C}_I^B = \{(x_1^B, y_1^B)^T, \dots, (x_I^B, y_I^B)^T\}$.

Remark 1 (The Role of Satellites): Satellite is a necessary component of the ATG network to enhance reliability, since pure ATG networks are inevitably influenced by various factors (e.g., weather conditions). In this work, we focus on the ATG communications network under the hybrid satellite–terrestrial network architecture, and the satellite is implicitly reflected for

---

[6]In practice, this can be conducted by uniformly sampling every route with a sufficiently large density, i.e., $\mathcal{C}^A = \{(x_1^A, y_1^A)^T, \dots, (x_Z^A, y_Z^A)^T\}$, where Z is the number of samples.

[7]Note that this ratio threshold can be properly set to control the BS construction cost. A too-large value of Ω may result in unnecessarily large value of I. For the locations where the QoS cannot be guaranteed by the ATG link, the aircraft turns to satellite as a supplement.

Algorithm 1: Stochastic Subgradient-Based BS Number and Location Optimization.

Require: Initial number of BSs I, number of iterations T, capacity requirement Ω, ratio of satisfying QoS Ψ, number of aircraft samples Z.

1: *loop:*
2: Randomly generate I BS locations $\mathbf{c}_I^B(0)$.
3: **for** $t = 0 : T$ **do**
4:      Randomly generate a new matrix of aircraft locations $\mathbf{c}^A = [(x_1^A, y_1^A)^T, \ldots, (x_J^A, y_J^A)^T]$ according to its distribution on considered routes.
5:      Calculate the average channel capacity C, and the capacity per aircraft C_j, based on the current aircraft and BS locations using (6)–(10).
6:      Calculate the derivatives of C and C_j with respect to $\mathbf{c}_I^B$ using (6)–(10), and obtain the subgradient $\mathbf{g_c}$ using (15)–(17).
7:      Calculate the corrected subgradient $\mathbf{S}(t)$ using (20).
8:      Calculate step length $\alpha(t)$ using (18)–(19).
9:      Update BS locations $\mathbf{c}_I^B = [(x_1^B, y_1^B)^T, \ldots, (x_I^B, y_I^B)^T]$ using (21).
10: **end for**
11: Calculate the corresponding capacity at each aircraft sampling place $\{C_1, \ldots, C_Z\}$, and statistical ratio that meets the communication rate $\psi = \frac{\sum (C_z \geqslant \Omega)}{Z}$.
12: **if** $\psi < \Psi$ **then**
13:     $I = I + 1$.
14:     **goto** *loop*.
15: **end if**
16: **return** $\mathcal{C}_I^B$ and I

the distribution of aircraft using ATG links on routes. Specifically, the effective capacity that can be provided by satellites, along with the weather statistics over the target routes, together affect the probability that an aircraft connects to an ATG BS. These probabilities measured on different routes will in turn affect the deployment of ATG BSs, as being reflected by the number and location of randomly generated aircraft on each route [i.e., $\mathbf{c}^A$ in (5) and (11)] when solving the problem.

Remark 2 (Adding New Routes): In practice, when newly planned routes are added into consideration, the BS location optimization needs to be conducted on the basis of existing BS locations (which have been optimized for the old routes only). For this case, Algorithm 1 can be slightly modified as follows. In Steps 2 and 9, the BS location matrix $\mathbf{c}_I^B$ is now expressed as

$$\mathbf{c}_I^B = \left[\mathbf{c}_{I_0}^{B_F}, \mathbf{c}_{I_*}^{B_D} \right] \quad (22)$$

where $\mathbf{c}_{I_0}^{B_F} = [(x_1^{B_F}, y_1^{B_F})^T, \ldots, (x_{I_0}^{B_F}, y_{I_0}^{B_F})^T]$ represents the fixed (i.e., already optimized for the old routes) BSs and $\mathbf{c}_{I_*}^{B_D} = [(x_1^{B_D}, y_1^{B_D})^T, \ldots, (x_{I_*}^{B_D}, y_{I_*}^{B_D})^T]$ represents the dynamic (i.e., to be optimized for the newly added routes) BSs. The fixed BSs will not participate in the iteration of the BS location update. As a result, the number of fixed BSs I_0 stays fixed in the iteration,

while only the number of dynamic BSs I_* will be increased in Step 13 of Algorithm 1

$$I_* = I_* + 1$$
$$I = I_0 + I_*. \quad (23)$$

The remaining procedure then follows the same steps as described in Algorithm 1.

IV. CLUSTERING ALGORITHM FOR UNIQUE BS LOCATION IDENTIFICATION

Due to the nonconvexity of problem (5), as well as the randomness introduced in stochastic optimization (e.g., random initialization of the BS locations in Step 4, and random generation of the aircraft locations in Step 6 of Algorithm 1), the obtained BS locations (and number) might be different in different runs of Algorithm 1. Examples are shown in Fig. 2, where Algorithm 1 has been independently conducted four times to cover five fixed routes. As demonstrated, in different runs of the algorithm, the resulted number of BSs is different (i.e., $I = 14$ for run #1, 16 for run #2, and 15 for run #3 and #4). Even when the algorithm outputs the same BS number, the optimized BS locations may also be different [see, e.g., Fig. 2(c) and (d)].

For practical implementation where a unique solution of the BS locations is required, we further adopt a clustering algorithm over the results obtained from multiple runs of Algorithm 1. Specifically, we first repeatedly and independently conduct Algorithm 1 for n times, resulting in a set of BS location coordinates $\mathcal{C}_\xi^B \triangleq \bigcup_{i=1}^n \mathcal{C}_{I_i}^B$. The cardinality of this set is $\xi = \sum_{i=1}^n I_i$. In the following, we apply the classic clustering algorithm (K-means[8]) over this location coordinates set, and use the obtained cluster centers as the final output for unique BS location determination.

K-means clustering requires predetermination of the number of clusters and initial cluster centers. For our considered scenario, we use the mean value of the BS number obtained with Algorithm 1 to determine K, i.e., $K = \lceil \frac{\xi}{n} \rceil$, whose symbol denotes rounding up. For the initialization of cluster centers, we set the initial locations of the BS cluster centers $\{\mathbf{p}_1, \mathbf{p}_2, \ldots \mathbf{p}_K\}$ to be evenly distributed on the routes. The number of BSs on each route is proportional to its length.

Then, we calculate the distances from each BS $\mathbf{c}_j$ in $\mathcal{C}_\xi^B$ to these cluster centers

$$d_{jk} = \|\mathbf{c}_j - \mathbf{p}_k\| \quad (24)$$

assign each BS to its nearest cluster center, and correspondingly obtain K clusters $\{\mathcal{Z}_1, \mathcal{Z}_2, \ldots, \mathcal{Z}_K\}$ where $\mathcal{Z}_i$ is the BS coordinates set associated with the ith cluster. New cluster centers $(\mathbf{p}_i^*, i = 1, \ldots, K)$ are then recalculated with $\{\mathcal{Z}_1, \mathcal{Z}_2, \ldots, \mathcal{Z}_K\}$

$$\mathbf{p}_i^* = \frac{1}{|\mathcal{Z}_i|} \sum_{\mathbf{p}_i \in \mathcal{Z}_i} \mathbf{p}_i \quad (25)$$

---

[8]Note that there exist many classic clustering methods, e.g., K-means [33], K-means++[34], DBSCAN [35], AGNES [36], etc. Via simulations, it is observed that the achieved performance difference between different clustering methods is not significant. Therefore, we choose K-means as an example to show how clustering can be conducted to finalize the proposed algorithm, for the reason that it is more convenient for implementation.
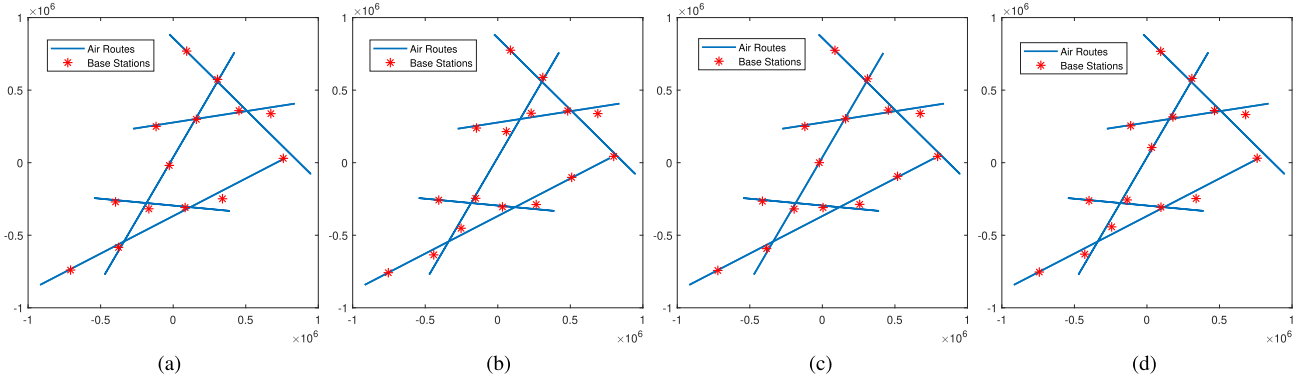
Fig. 2. Outputs of Algorithm 1 for four independent runs. (a) Run #1 ($I = 14$). (b) Run #2 ($I = 16$). (c) Run #3 ($I = 15$). (d) Run #4 ($I = 15$).

and used to form new clusters from $\mathcal{C}_{\xi}^{B}$. The above procedure is conducted iteratively, until the variation between the cluster centers obtained in the last two iteration steps

$$\theta \triangleq \sum_{i=1}^{K} \|\mathbf{p}_i^* - \mathbf{p}_i\| \tag{26}$$

is less than a certain threshold Θ.

Through the clustering algorithm, the BSs can be automatically divided into K clusters whose centers $\{\mathbf{p}_1^*, \mathbf{p}_2^*, \ldots, \mathbf{p}_K^*\}$ are used for practical BS location determination.

V. SIMULATION RESULTS

In this section, we provide simulation results to validate the effectiveness of the proposed algorithms. As an example, we consider five realistic routes[9] shown in Fig. 3 and deploy BSs to meet the communication demands on these routes. We assume that both the aircraft and the BS are equipped with multiple antennas, and the ratio of aircraft antenna to BS antenna is $\beta = 1/8$. The maximum number of aircraft on every route, according to the route length, is set to $\{\overline{J_1}, \overline{J_2} \ldots, \overline{J_5}\} = \{30, 25, 20, 25, 15\}$, respectively. To guarantee flight safety, we assume that the distance between any two aircraft is no less than 40 km. To ensure such a requirement, in every iteration of Algorithm 1, we first randomly generate a corresponding number of aircraft on the routes, then the aircraft locations that do not satisfy the safety distance requirement are discarded (as a result, the number of aircraft might be different for each iteration). After that, the total number of remaining aircraft is $J = \sum_{i=1}^{5} J_i$, where J_i is the number of remaining aircraft on the ith route. The initial number of BSs is set to be $I = 10$, with their initial locations randomly generated in the considered area. The specific parameters of the algorithm are given in Table I.
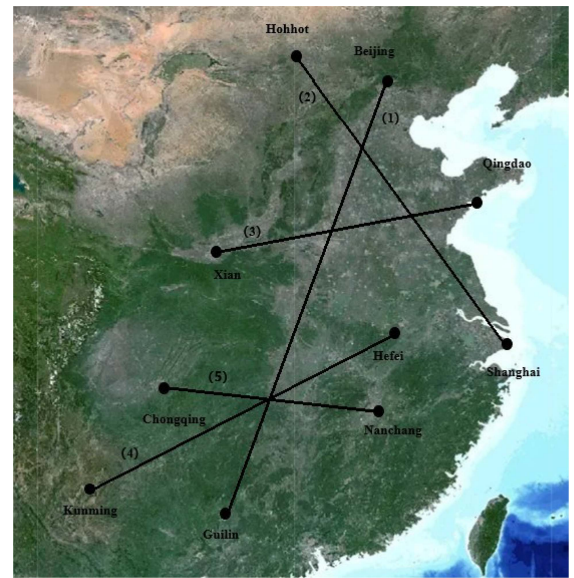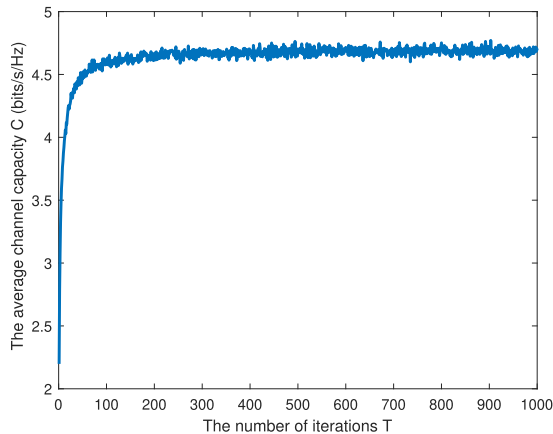

Fig. 3. Five realistic routes in China. (1) Beijing to Guilin. (2) Shanghai to Hohhot. (3) Qingdao to Xi'an. (4) Kunming to Hefei. (5) Chongqing to Nanchang.
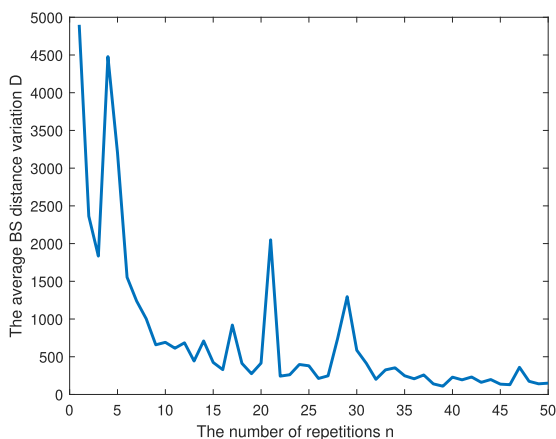
TABLE I
SIMULATION PARAMETERS

Parameter	Value	Parameter	Value
d_0	1 m	Ω	2 bits/s/Hz
n_0	2	Z	700
c	3×10^8 m/s	β	1/8
f	973 MHz	a	7500
P	53 dBm	b	0.8
σ_0^2	−174 dBm/Hz	Ψ	95%

A. Algorithm Convergence

We first evaluate the convergence performance of our proposed algorithms. The convergence of Algorithm 1 is shown in Fig. 4(a), where the average channel capacity C (averaged over 2000 independent runs of Algorithm 1) is depicted versus the number of iterations T. As shown, Algorithm 1 converges fast to a stable output of C. According to the result, we set the total number of iterations T to 400 in the following simulations.

---

[9]For more scenarios with randomly generated air routes, it has also been validated via simulations, that the proposed algorithm is able to achieve a superior performance. Therefore, its robustness to different route distributions is guaranteed.

(a)

(b)

Fig. 4. Convergence performance of the proposed algorithms. (a) Convergence of Algorithm 1: Average channel capacity C versus Number of iterations T. (b) Convergence of K-means algorithm: Average BS distance variation D versus Number of repetitions n.

Next, we demonstrate the convergence of the BS location clustering algorithm in Fig. 4(b). In the simulation, Algorithm 1 is conducted independently for n times (the x-axis) to generally enrich the BS location set $\mathcal{C}_\xi^B$. For every value of n, the K-means clustering algorithm is conducted, to obtain a unique result $\mathbf{p}(n)$ for the BS deployment under the current $\mathcal{C}_\xi^B$. We use the average BS distance variation to show the convergence of the above clustering algorithm, which is defined as $D(n) = \frac{1}{K} \sum_{i=1}^{K} d_i(n)$, where $d_i(n) = \|\mathbf{p}_i(n+1) - \mathbf{p}_i(n)\|$ is the location difference of the ith BS, measured between the nth and the $(n+1)$th iteration steps. As shown in Fig. 4(b), the K-means clustering algorithm demonstrates rapid convergence. Although fluctuations are observed during the convergence process, these can be attributed to the randomness of the initial state during the iteration process, which may lead to differences in the obtained results (such as the number and location of BSs) and shift the clustering center. Nevertheless, these changes tend to smoothen as the number of iterations increases. The average variation in BS distance tends to stabilize after 30 repetitions, where the parameter D becomes less than 1 km. This value is considered
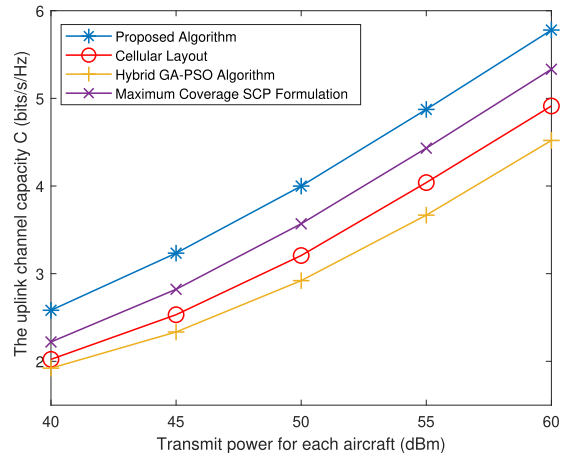

Fig. 5. Uplink channel capacity C versus transmit power.

insignificant in comparison to the expansive coverage of the entire route map.

B. Performance Comparison

In the following, we compare the performances obtained with the different BS location planning methods. Aside from the proposed algorithm, we consider the following baseline approaches.

1) Cellular layout [7]: The entire area is divided according to a traditional honeycomb pattern, and the BSs are deployed in the center of the cells above which there exist routes passing through.
2) Hybrid GA-PSO algorithm [25].
3) Maximum coverage SCP formulation [26].

We first compare the average uplink capacity achieved with these four methods in Fig. 5. Significantly, the proposed algorithm outperforms the other baseline methods. Note that the results in Fig. 5 are averaged over all possible aircraft locations along the routes. To gain more details on the average capacity distribution for aircraft at different locations, we further illustrate the cumulative distribution function (CDF) curves of the uplink capacity in Fig. 6. The empirical CDF is obtained by randomly generating 1000 groups of aircraft on the considered routes and correspondingly calculating the capacity achieved at every group of aircraft locations. As observed, the CDF curve of the proposed algorithm lies at the right-hand side of that of the baseline methods, indicating that the proposed BS location optimization has merit in improving the capacity not only in the average sense, it is beneficial, statistically, for all outage capacities.

At last, we focus on one aircraft and show its capacity changing during the flight. Consider an aircraft flying from Beijing to Guilin, i.e., it flies along the route (1) in Fig. 3. The uplink capacity of the aircraft is shown against its flight distance in Fig. 7. The peaks in the curves indicate that the aircraft flies above (or nearby) an ATG BS at those corresponding locations. As shown in Fig. 7, we can conclude that compared with other methods, the hybrid GA-PSO algorithm deploys fewer BSs around the route (1). As well as the cellular layout has lower peak capacities
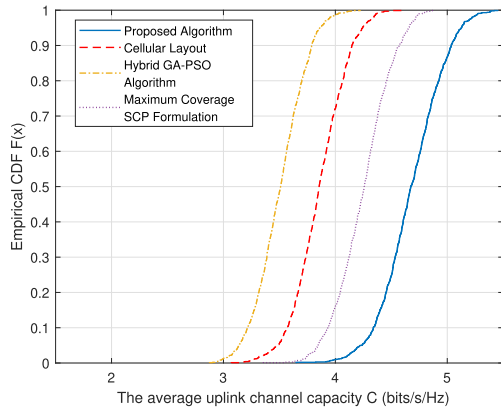
Fig. 6. Empirical CDF of the uplink capacity achieved along the considered routes.
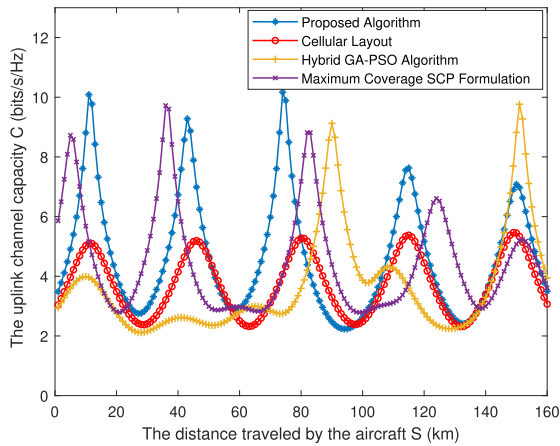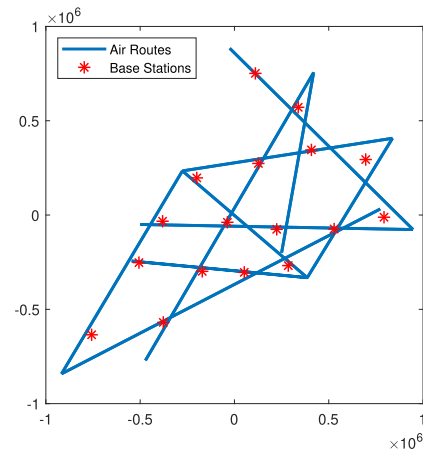

(a)

Fig. 7. Instantaneous capacity changing when one aircraft is flying along its route.

(b)

Fig. 8. Optimized BS locations when new routes are added. (a) Fully replanned layout. (b) Partially replanned layout.

since its BS deployment does not fully exploit the information of the routes. Maximum coverage SCP formulation, on the other hand, has high peak capacities but performs unsatisfactorily in the intermediate regions between its adjacent BSs. Notably, the proposed algorithm outperforms the other methods, in terms of both the peak capacity and the intermediate region coverage.
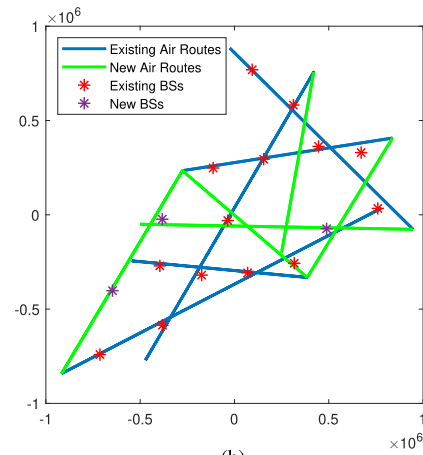
To summarize, through the above simulations, it can be confirmed that the proposed BS location optimization method is beneficial in enhancing the average capacity of the entire ATG communications network, improving the random capacity distribution over the considered routes, as well as providing better instantaneous service for an aircraft during its flight along the corresponding route.

C. Adding New Routes

At last, we evaluate the performance of the proposed algorithm for the practical scenario described in Remark 2. That is, new routes are added on the basis of the old routes. New BSs need to be deployed to cover these new routes, and their locations now have to be optimized in the presence of existing BSs (which

have already been optimized and deployed according to the old routes).

We add five new routes into the scenario previously described in Fig. 3, where five old routes already exist. In addition to the compared methods, we apply the proposed algorithm to two cases. 1) Fully replanned layout, which conducts our proposed algorithms overall ten routes, that is, the locations of old BSs will no longer be considered in such a process. Although this is not realistic, the method serves as a performance upper bound to show the performance loss stemming from the more practical partially re-plan approach. 2) Partially replanned layout, which optimizes the locations of newly added BSs only, on the basis of existing BSs. This method is conducted following the procedure previously described in Remark 2.

We first demonstrate and compare the BS locations obtained with the fully replan and partially replan approaches, respectively. As can be observed in Fig. 8, the partially replanned BS locations distribute less evenly than that obtained with the fully replan, due to the lack of the degrees of freedom in its design. To compare their performances more directly, we further show the CDF of uplink capacity achieved with the considered schemes in
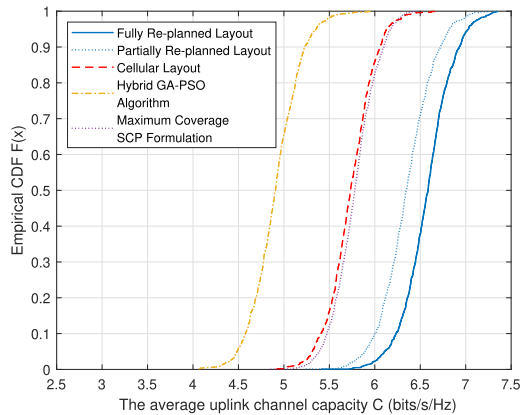
Fig. 9. Empirical CDF of the uplink capacity achieved along the considered routes (adding new routes).

Fig. 9. The simulation is conducted following the same process as that has been described in Fig. 6. Although the partially replan approach has slightly lower capacity over the routes compared to fully replan, it still shows clear advantage compared with the other methods. This confirms the effectiveness of applying the proposed algorithms for BS location planning in realistic scenarios, where new routes will be continuously added with the fast development of the aviation industry.

VI. Conclusion

We aimed to obtain the optimal number and locations of ATG BSs to maximize the perantenna uplink channel capacity, while as much as possible guaranteeing QoS of all aircraft along the target routes with minimum cost. We proposed a stochastic-based gradient algorithm to solve the problem, where the solution could be nonunique due to the nonconvexity of the problem, as well as the randomness introduced in stochastic optimization. To tackle such the nonuniqueness issue, we further proposed to apply the clustering method (K-means) to obtain a unique solution of the BS number and locations for practical implementation. Simulations were conducted to show the advantage of the proposed algorithms over other baseline methods, in terms of both the average capacity and the capacity distribution, as well as the instantaneous capacity achieved by an aircraft flying along its route. At last, the effectiveness of the proposed algorithm was further shown in a realistic scenario where new routes were added on the basis of the old ones.
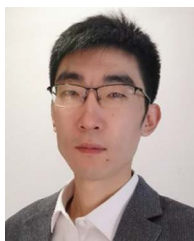
References

[1] A. Jahn et al., "Evolution of aeronautical communications for personal and multimedia services," *IEEE Commun. Mag.*, vol. 41, no. 7, pp. 36–43, Jul. 2003.

[2] G. G. McGrath, "An optimization metric for air-to-ground network planning," *IEEE Trans. Wireless Commun.*, vol. 8, no. 5, pp. 2336–2340, May 2009.

[3] W. Feng et al., "Radio map-based cognitive satellite-UAV networks towards 6G on-demand coverage," *IEEE Trans. Cogn. Commun. Netw.*, early access, Dec. 22, 2023, doi: 10.1109/TCCN.2023.3345857.

[4] Y. Wang, W. Feng, J. Wang, and T. Q. S. Quek, "Hybrid satellite-UAV-terrestrial networks for 6G ubiquitous coverage: A maritime communications perspective," *IEEE J. Sel. Areas Commun.*, vol. 39, no. 11, pp. 3475–3490, Nov. 2021.

[5] C. Liu, W. Feng, Y. Chen, C.-X. Wang, and N. Ge, "Cell-free satellite-UAV networks for 6G wide-area Internet of Things," *IEEE J. Sel. Areas Commun.*, vol. 39, no. 4, pp. 1116–1131, Apr. 2021.

[6] X. Fang et al., "NOMA-based hybrid satellite-UAV-terrestrial networks for 6G maritime coverage," *IEEE Trans. Wireless Commun.*, vol. 22, no. 1, pp. 138–152, Jan. 2023.

[7] D. Zhou, M. Sheng, J. Li, and Z. Han, "Aerospace integrated networks innovation for empowering 6G: A survey and future challenges," *IEEE Commun. Surveys Tuts.*, vol. 25, no. 2, pp. 975–1019, Apr.–Jun., 2023.

[8] S. Sharif, S. Zeadally, and W. Ejaz, "Space-aerial-ground-sea integrated networks: Resource optimization security in 6G networks," in *Proc. IEEE Mil. Commun. Conf.*, 2022, pp. 7–12.

[9] S. Li, Q. Chen, W. Meng, and C. Li, "Civil aircraft assisted space-air-ground integrated networks: An innovative NTN of 5G and beyond," *IEEE Wireless Commun.*, vol. 29, no. 4, pp. 64–71, Aug. 2022.

[10] S. Li, Q. Chen, Z. Li, W. Meng, and C. Li, "Civil aircraft assisted space-air-ground integrated networks: Architecture design and coverage analysis," *China Commun.*, vol. 19, no. 1, pp. 29–39, Jan. 2022.

[11] Q. Chen, W. Meng, S. Han, C. Li, and H.-H. Chen, "Reinforcement learning-based energy-efficient data access for airborne users in civil aircrafts-enabled SAGIN," *IEEE Trans. Green Commun. Netw.*, vol. 5, no. 2, pp. 934–949, Jun. 2021.

[12] Q. Fang, W. Tian, X. Zhou, and J. Yang, "Evaluation of air route network congestion based on node importance," in *Proc. Integr. Commun. Navigation Surveill. Conf.*, 2022, pp. 1–9.

[13] G. Tian, T. Shang, Q. Zhang, K. Cai, and L. Zhao, "Lightweight group pre-handover authentication scheme for aviation 5G air-to-ground networks," in *Proc. 19th Int. Conf. Wireless Mobile Comput. Netw. Commun.*, 2023, pp. 324–329.

[14] A. Papa, J. V. Mankowski, H. Vijayaraghavan, B. Mafakheriy, L. Gorattiy, and W. Kellerer, "Enabling 6G applications in the sky: Aeronautical federation framework," *IEEE Netw.*, early access, Mar. 7, 2023, doi: 10.1109/MNET.132.2200526.

[15] L. Li, B. Ma, Z. Jia, and Y. Si, "Base station locations optimization in LTE using artificial immune algorithm," in *Proc. 10th Int. Symp. Comput. Intell. Des.*, 2017, pp. 165–168.

[16] N. A. A. Latiff and I. S. Ismail, "Performance of mobile base station using genetic algorithms in wireless sensor networks," in *Proc. German Microw. Conf.*, , pp. 251–254.

[17] H. Wang, W. Huangfu, Y. Liu, C. Gong, Y. Ren, and W. Liu, "Spatial feature aware genetic algorithm of network base station configuration for Internet of Things," in *Proc. 6th Int. Symp. Comput. Netw. Workshops*, 2018, pp. 53–58.

[18] Y. Li and C. Zhang, "Analytic comparisons of the high-speed railway base station arrangement strategy in fading channels," in *Proc. Int. Workshop High Mobility Wireless Commun.*, 2014, pp. 178–182.

[19] C. Zhang et al., "Service based high-speed railway base station arrangement," *Wireless Commun. Mobile Comput.*, vol. 15, no. 13, pp. 1681–1694, 2015.

[20] A. Shaverdian, S. Shahsavari, and C. Rosenberg, "Air-to-ground cellular communications for airplane maintenance data offloading," *IEEE Trans. Veh. Technol.*, vol. 71, no. 10, pp. 11060–11077, Oct. 2022.

[21] E. Dinc, M. Vondra, and C. Cavdar, "Multi-user beamforming and ground station deployment for 5G direct air-to-ground communication," in *Proc. IEEE Glob. Commun. Conf.*, 2017, pp. 1–7.

[22] E. Dinc, M. Vondra, and C. Cavdar, "Total cost of ownership optimization for direct air-to-ground communication networks," *IEEE Trans. Veh. Technol.*, vol. 70, no. 10, pp. 10157–10172, Oct. 2021.

[23] V. Towhidlou, S. Al-Rubaye, and A. Tsourdos, "LTE handover design for cellular-connected aircraft," in *Proc. IEEE/AIAA 41st Digit. Avionics Syst. Conf.*, 2022, pp. 1–5.

[24] *5G White Paper*, Feb. 2015. Accessed: Feb. 15, 2023. [Online] Available: https://www.ngmn.org/work-programme/5g-white-paper.html

[25] B. Cao, W. Liu, B. Li, and K. Liu, "ADS-B ground station site selection analysis based on intelligent algorithm," in *Proc. IEEE 2nd Int. Conf. Civil Aviation Saf. Inf. Technol.*, 2020, pp. 686–690.

[26] N. Wang, D. Delahaye, A. Gondran, and M. Mongeau, "Automatic dependent surveillance-broadcast ground-station optimal deployment problem," *J. Air. Transp.*, vol. 26, no. 3, pp. 104–112, Aug. 2018.

[27] J. Naganawa and H. Miyazaki, "Opportunistic-target-measurement-based narrowband statistical modeling of civil aviation surveillance signal at 1090 MHz," *IEEE Trans. Antennas Propagat.*, vol. 68, no. 3, pp. 2304–2314, Mar. 2020.

[28] Y. Zhang and L. Dai, "A closed-form approximation for uplink average ergodic sum capacity of large-scale multi-user distributed antenna systems," *IEEE Trans. Veh. Technol.*, vol. 68, no. 2, pp. 1745–1756, Feb. 2019.

[29] D. Aktas, M. N. Bacha, J. S. Evans, and S. V. Hanly, "Scaling results on the sum capacity of cellular networks with MIMO links," *IEEE Trans. Inf. Theory*, vol. 52, no. 7, pp. 3264–3274, Jul. 2006.

[30] J. Papandriopoulos and J. S. Evans, "Low-complexity distributed algorithms for spectrum balancing in multi-user DSL networks," in *Proc. IEEE Int. Conf. Commun.*, 2006, pp. 3270–3275.

[31] B. Stephen and A. Mutapcic, "Stochastic subgradient methods," *Lecture Notes for EE364b*, Stanford Univ., Stanford, CA, USA, 2008.

[32] I. Goodfellow et al. *Deep Learning*, vol. 1. Cambridge, MA, USA:MIT Press, 2016.

[33] J. AnilK, "Data clustering: 50 years beyond K-Means," *Pattern Recognit. Lett.*, vol. 31, no. 8, pp. 651–666, 2010.

[34] A. Kapoor and A. Singhal, "A comparative study of K-means, K-means and fuzzy C-means clustering algorithms," in *Proc. 3rd Int. Conf. Comput. Intell. Commun. Technol.*, 2017, pp. 1–6.

[35] K. Khan, S. U. Rehman, K. Aziz, S. Fong, and S. Sarasvady, "DBSCAN: Past, present and future," in *Proc. 5th Int. Conf. Appl. Digit. Inf. Web Technol.*, 2014, pp. 232–238.

[36] R. J. Gil-Garcia, J. M. Badia-Contelles, and A. Pons-Porrata, "A general framework for agglomerative hierarchical clustering algorithms," in *Proc. 18th Int. Conf. Pattern Recognit.*, 2006, pp. 569–572.

Ruifeng Gao (Member, IEEE) received the B.S. degree in geo-information science and technology from Central South University, Changsha, China, in 2009, and the M.S. degree in communication and information system and the Ph.D. degree in information and communication engineering from Nantong University, Nantong, China, in 2013 and 2019, respectively.

From 2019 to 2020, he was a Visiting Scholar with the Singapore University of Technology and Design, Singapore. He is currently an Associate Professor with the School of Transportation and Civil Engineering, Nantong University. His research interests include maritime communication networks, resource management, and machine learning.

Qinzhao Zhang received the B.S. degree in communication engineering from Xidian University, Xi'an, China, in 2018. He is currently working toward the M.A.Eng. degree in electronic information with the Department of Electronic Engineering, Tsinghua University, Beijing, China.

His research interests include ATG communications, hybrid satellite–terrestrial networks, and beamforming.

Yanmin Wang received the B.S. degree from Shandong University, China, in 2008, and the Ph.D. degree in information and communication engineering from Tsinghua University, Beijing, China, in 2013.

She is currently an Associate Professor with the School of Information Engineering, Minzu University of China, Beijing. Her research interests include distributed antenna systems, satellite networks, and coordinated satellite-UAV-terrestrial networks.

Jue Wang (Member, IEEE) received the B.S. degree in communications engineering from Nanjing University, Nanjing, China, in 2006, the M.S. and Ph.D. degrees in information and communication engineering from National Communications Research Laboratory, Southeast University, Nanjing, in 2009 and 2014, respectively.

From 2014 to 2016, he was a Postdoctoral Research Fellow with the Singapore University of Technology and Design, Singapore. He is currently with the School of Information Science and Technology, Nantong University, Nantong, China. His research interests include MIMO/Massive MIMO wireless communications, nonterrestrial networks, and machine learning in communication systems.

Dr. Wang has been a Technical Program Committee Member and a Reviewer for a number of IEEE conferences/journals. He was the recipient of Exemplary Reviewer of IEEE TRANSACTIONS ON COMMUNICATIONS in 2014, and Exemplary Reviewer of IEEE WIRELESS COMMUNICATIONS LETTERS in 2021.

Wei Feng (Senior Member, IEEE) received the B.S. and Ph.D. degrees in information and communication engineering from Tsinghua University, Beijing, China, in 2005 and 2010, respectively.

He is currently a Professor with the Department of Electronic Engineering, Tsinghua University. His research interests include maritime communication networks, large-scale distributed antenna systems, and coordinated satellite-UAV-terrestrial networks.

Dr. Feng is currently an Assistant to the Editor-in-Chief of *China Communications*. He is also the Editor of IEEE TRANSACTIONS ON COGNITIVE COMMUNICATIONS AND NETWORKING.